

Accelerated Publications

Identification of Histidine 77 as the Axial Heme Ligand of Carbonmonoxy CooA by Picosecond Time-Resolved Resonance Raman Spectroscopy[†]

Takeshi Uchida,[‡] Haruto Ishikawa,[§] Koichiro Ishimori,[§] Isao Morishima,^{*,§} Hiroshi Nakajima,^{||} Shigetoshi Aono,^{*,||} Yasuhisa Mizutani,[‡] and Teizo Kitagawa^{*,‡}

Institute for Molecular Science, Okazaki National Research Institutes, Myodaiji, Okazaki 444-8585, Japan, Department of Molecular Engineering, Graduate School of Engineering, Kyoto University, Kyoto 606-8501, Japan, and School of Materials Science, Japan Advanced Institute of Science and Technology, 1-1 Asahidai, Tatsunokuchi, Nomi-gun, Ishikawa 923-1292, Japan

Received May 22, 2000; Revised Manuscript Received August 22, 2000

ABSTRACT: The heme proximal ligand of carbonmonoxy CooA, a CO-sensing transcriptional activator, in the CO-bound form was identified to be His77 by using picosecond time-resolved resonance Raman spectroscopy. On the basis of the inverse correlation between Fe–CO and C–O stretching frequencies, we proposed previously that His77 is the axial ligand trans to CO [Uchida et al. (1998) *J. Biol. Chem.* 273, 19988–19992], whereas later a possibility of displacement of His77 by CO with retention of another unidentified axial ligand was reported [Vogel et al. (1999) *Biochemistry* 38, 2679–2687]. Although our previous resonance Raman study failed to detect the Fe–His stretching [$\nu(\text{Fe–His})$] mode of CO-photodissociated CooA of the carbonmonoxy adduct due to the rapid recombination, application of the picosecond time-resolved resonance Raman technique enabled us to observe a new intense line assignable to $\nu(\text{Fe–His})$ at 211 cm^{-1} immediately after photolysis, while it became nondiscernible after 100-ps delay. The low $\nu(\text{Fe–His})$ frequency of photodissociated CooA indicates the presence of some strain in the Fe–His bond in CO-bound CooA. This and the rapid recombination of CO characterize the heme pocket of CooA. The 211 cm^{-1} band was completely absent in the spectrum of the CO-photodissociated form of the His77-substituted mutant but the Fe–Im stretching band was observed in the presence of exogenous imidazole (Im). Thus, we conclude that His77 is the axial ligand of CO-bound CooA and CO displaces the axial ligand trans to His77 with retention of ligated His77 to activate CooA as the transcriptional activator.

CooA, a newly discovered CO-sensing hemoprotein, acts as a transcriptional activator for the expression of a CO

[†] This work was supported by Grants-in-Aid for Scientific Research on Priority Areas, Molecular Biometallics, from the Ministry of Education, Science, Sports and Culture: 08249102 to I.M., 09235212 to S.A., and 08249106 to T.K. T.U. and H.I. were supported by fellowships from the Japan Society for Promotion of Science to Japanese young scientists.

* Authors to whom correspondence should be addressed. T.K.: phone, +81-564-55-7340; fax, +81-564-55-4639; e-mail, teizo@ims.ac.jp. S.A.: phone, +81-761-51-1681; fax, +81-761-51-1149; e-mail, aono@jaist.ac.jp. I.M.: phone, +81-75-753-5921; fax, +81-75-751-7611; e-mail, morisima@mds.moleng.kyoto-u.ac.jp.

[‡] Okazaki National Research Institutes.

[§] Kyoto University.

^{||} Japan Advanced Institute of Science and Technology.

oxidation system in *Rhodospirillum rubrum* (1–4) and works as a homodimeric protein containing one six-coordinate (6c) low-spin heme per subunit (5–8). By analogy with one of the well-known transcriptional regulators from *Escherichia coli*, CRP¹ (9), CooA is supposed to have two functional domains, i.e., the N-terminal heme-binding and C-terminal DNA-binding domains (10). Carbon monoxide binds only to the ferrous heme and is considered to cause some conformational changes that trigger the specific binding of CooA on its target DNA (2, 10).

To elucidate the molecular mechanism for the transcriptional activator activity of CooA, it is essential to explore the structural change of the heme moiety upon CO binding. Previous spectroscopic and mutational studies (5, 7, 8) have revealed the ferrous heme of CooA in the absence of CO to be six-coordinated. One of axial ligands is undoubtedly His77 but the other axial ligand (X) has not yet been identified. In the presence of CO, the UV–visible spectrum of CooA is changed to that of a typical CO-ligated hemoprotein such as carbonmonoxy Hb and Mb (2, 4, 5, 7), indicating that one of the axial ligands of the ferrous heme iron is replaced with CO, while a nitrogenous ligand is retained.

We previously reported the RR spectra of CooA in the presence of CO (6), proposing that the axial ligand in the CO-bound form is a neutral histidine on the basis of the well-known inverse correlation between the frequencies of the Fe–CO [$\nu(\text{Fe–C})$] and C–O stretching [$\nu(\text{C–O})$] modes (11). Combined with the mutational studies, it was concluded that His77 is the axial ligand for CO-bound CooA (5, 6). On the other hand, Roberts and co-workers compared the RR spectra of CooA in the presence and absence of CO and raised a possibility that CO displaces His77, leaving X on the heme iron (8). They found close similarity in the MCD spectra as well as the RR spectra between the wild-type and H77Y mutant protein (His77 \rightarrow Tyr), which led them to propose that His77 is displaced by CO with retention of X (12).

To identify the axial ligand of CO-bound CooA, we have tried to detect the Fe–His stretching mode [$\nu(\text{Fe–His})$] in the photoproduct of CO-bound CooA. However, the geminate rebinding of CO in CooA was quite fast, which prevented us from observing the $\nu(\text{Fe–His})$ mode in a photo-steady state under CW irradiation (6). To observe it, in this study, we applied picosecond time-resolved RR spectroscopy (13). Heme-bound CO was photodissociated by a picosecond laser pulse, and vibrations of the transiently formed five-coordinate (5c) species were monitored by the subsequent picosecond probe pulse. RR spectra of the H77Y mutant in the presence and absence of exogenous imidazole (Im) were also examined. The results thus obtained revealed unambiguously that CO-bound CooA has His77 as the axial ligand and CO binds to the heme iron with dissociation of another axial ligand trans to His77, which would induce the conformational changes of the whole protein to trigger the activation of CooA.

EXPERIMENTAL PROCEDURES

Overexpression of CooA followed the protocols of Aono et al. (4). In this work we used the *E. coli* BL21 or JM109

strain as a host for the expression of CooA. *E. coli* BL21 was used to avoid the degradation of the expressed CooA by proteases. Wild-type and H77Y mutant CooA were purified according to the methods of Aono et al. (4, 5) or Shelper et al. (2) with some modification. These two protocols gave the identical result. All kinds of column chromatography were performed with an FPLC system (Amersham Pharmacia). Purified CooA was dissolved in 50 mM Tris–HCl buffer (pH 8.0). The purity of this preparation was confirmed by SDS–PAGE to be ca. 95%. The CO-bound CooA was prepared by adding sodium dithionite solution to the purified protein solution with the final concentration of 4 mM, followed by anaerobic introduction of gaseous CO.²

Details of the picosecond time-resolved RR measurement system were described previously (13, 14). The probe beam at 442 nm (4 μJ) was generated as the first Stokes line in stimulated Raman scattering from CH₄ gas, and the pump beam at 559 nm (23 μJ) was generated with a home-built optical parametric generator and amplifier. Both were produced from the second harmonic of the 784 nm output of a Ti–sapphire laser operated at 1 kHz. The scattered light was detected with a liquid nitrogen cooled CCD detector (CCD-1100PB, Princeton Instruments), which was attached to a single spectrograph (500IM-CM, Chromex). The sample cell was rotated during data collection so that each photolyzing laser pulse can illuminate a fresh volume of sample. Raman shifts were calibrated with CCl₄ and cyclohexane.

RESULTS

Figure 1 depicts the time-resolved RR difference spectra in the low-frequency region of CO-bound CooA at –5, 5, 50, 100, and 1000 ps after photolysis which were obtained by subtracting the probe-only spectrum from the pump–probe spectra. The probe-only spectrum, which is displayed at the bottom in Figure 1, has no peak at 211 cm^{–1} but has a strong ν_7 band at 670 cm^{–1}. In the spectrum for the delay time of –5 ps, there are no bands between 200 and 800 cm^{–1}, which indicates that the pump–probe spectrum observed before photolysis is identical with that of the steady state of CO-bound CooA. In contrast, at 5-ps delay after photolysis, a new intense band appeared at 211 cm^{–1}.³ This band was also observed at 50- and 100-ps delays with decreasing intensity and completely disappeared at 1000 ps after photolysis. Since the $\nu(\text{Fe–His})$ band is observable in the 200–250 cm^{–1} region only for 5c reduced hemes (15), we tentatively assigned the transient band at 211 cm^{–1} to the Fe–His stretching mode.

To confirm that the 211 cm^{–1} band is derived from the photodissociated 5c CooA, the other marker band, ν_4 , was examined. The ν_4 band usually appears at 1355 cm^{–1} for

¹ Abbreviations: CRP, cyclic AMP receptor protein; Hb, hemoglobin; Mb, myoglobin; RR, resonance Raman; DTT, dithiothreitol; sGC, soluble guanylate cyclase; Im, imidazole.

² Previous studies (2, 7, 8) have reported that H77Y is difficult to reduce and that dithionite reduction produces a mixture of the ferric and ferrous forms. However, the electronic absorption and resonance Raman spectra of the reduced and CO-bound H77Y mutant produced in this way indicated that the mutant protein was completely reduced (data not shown). A relatively higher concentration of dithionite solution and/or the absence of DTT might contribute to the full conversion of the ferric H77Y mutant into the reduced form.

³ The peak frequencies of the Fe–His stretching modes were determined by fitting the spectra to a Gaussian function.

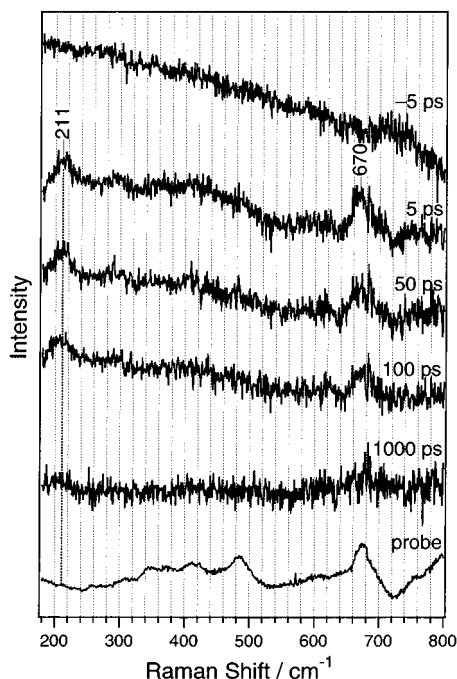


FIGURE 1: Time-resolved resonance Raman spectra of photodissociated CoxA-CO in the low-frequency region for time delays at -5 , 5 , 50 , 100 , and 1000 ps and the probe-only spectrum of CoxA-CO (bottom). The time-resolved spectra were obtained by subtracting the probe-only spectrum from the observed pump-probe spectra with an appropriate factor. The protein is in 50 mM Tris-HCl, pH 8.0 at room temperature. Experimental conditions: enzyme concentration, 200 μ M; pump beam, 559 nm and 23 μ J; probe beam 442 nm and 4 μ J (both 1 kHz). The total accumulation time for each spectrum was 5 min.

the $5c$ species, such as deoxy Mb (16), whereas it appears at 1360 – 1373 cm^{-1} for the $6c$ species (17–19). This frequency becomes higher when the sixth ligand is a π acceptor like O_2 and CO. Figure 2 shows the time-resolved RR difference spectra in the high-frequency region of CO-bound CoxA from -5 to 1000 -ps delay after photolysis. The probe-only spectrum, which is displayed at the bottom, gives a single ν_4 band at 1372 cm^{-1} . The absence of a peak at 1355 cm^{-1} corroborates that no photodissociation takes place by the probe beam. After the photolysis, however, a clear RR band was found at 1353 cm^{-1} . This frequency of ν_4 is that of a typical $5c$ species with a nitrogenous axial ligand (not sulfur anion). The Raman band at 1353 cm^{-1} becomes weaker with time and is completely absent at 1000 ps after photolysis, in agreement with the temporal behavior of intensity of the 211 cm^{-1} band (Figure 1). Thus, it can be unambiguously deduced that the 211 cm^{-1} band observed at 5 – 200 -ps delay after the photolysis is derived from the Fe-His stretching mode of the photodissociated $5c$ CoxA. Since the photoproducts of hemoproteins in the picosecond time regime are not considered to switch the axial ligand of the heme from that before the photolysis (13, 20), we conclude that CO-bound CoxA has a histidine residue as the axial ligand trans to CO.

To further confirm the axial coordination of histidine in CO-bound CoxA, we investigated a histidine mutant of CoxA, H77Y, in which His77 was replaced with Tyr. The absorption spectrum of the CO-bound form of H77Y CoxA (not shown) was the same as that reported (5), and its RR spectrum in the low-frequency region is delineated by trace A in Figure 3, which resembles the spectrum reported by

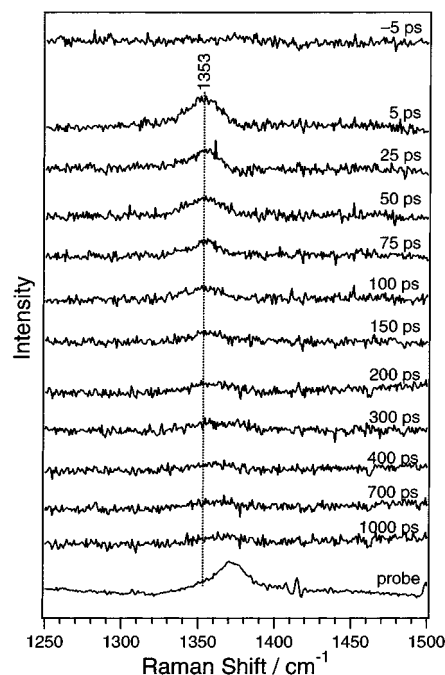


FIGURE 2: Time-resolved resonance Raman spectra of photodissociated CoxA-CO in the high-frequency region for time delays from -5 to 1000 ps and the probe-only spectrum of CoxA-CO (bottom). The spectra were obtained by subtracting the probe-only spectrum from the pump-probe spectra with an appropriate factor. Sample and experimental conditions are the same as those for Figure 1.

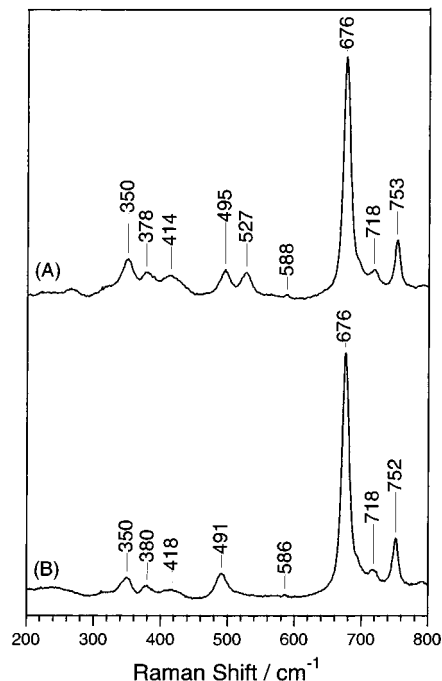


FIGURE 3: Stationary-state resonance Raman spectra of the H77Y mutant of CoxA-CO in the absence (A) and presence (B) of exogenous imidazole (100 mM). Experimental conditions are the same as those for Figure 1 except for the absence of the pump beam.

Vogel et al. (8). Two CO-isotope-sensitive bands (8) are seen at 495 and 527 cm^{-1} in Figure 3. The former and latter are assigned to the $\nu(\text{Fe}-\text{C})$ modes of the $6c$ and $5c$ adducts, respectively, although the trans ligand of CO in the $6c$ species cannot be specified. The occurrence of CO photodissociation for both species was confirmed from flash photolysis

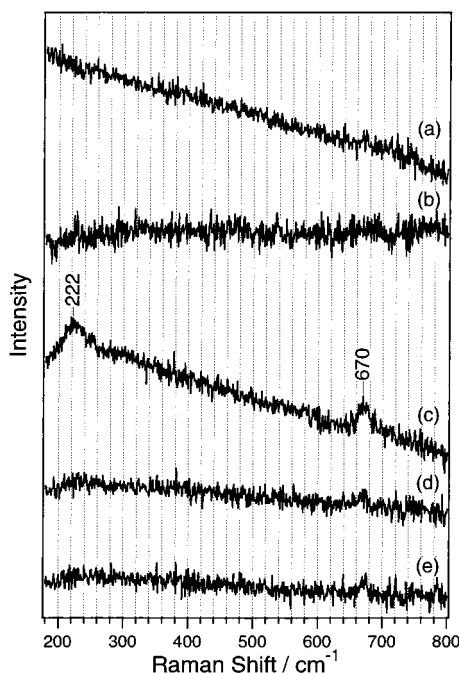


FIGURE 4: Time-resolved resonance Raman spectra of the photodissociated H77Y mutant of CoxA in the same frequency region as that of Figure 3 for time delays of -10 ps (a) and $+10$ ps (b) in the absence of exogenous imidazole and for time delays of $+10$ ps (c), $+100$ ps (d), and $+1000$ ps (e) in the presence of 100 mM imidazole. Sample and experimental conditions are the same as those of Figure 1 except for addition of imidazole.

experiments (not shown). When a 500 -fold molar excess of imidazole was added to this sample, the band corresponding to the $5c$ species disappeared while the band of the $6c$ species was shifted to 491 cm^{-1} , as displayed by trace B in Figure 3.

The time-resolved RR spectra in the same frequency region of the photodissociated H77Y CoxA-CO in the absence of imidazole are shown in Figure 4a,b, which were obtained for the delay times of -10 and 10 ps, respectively. In contrast with those of wild-type CoxA shown in Figure 1, there are no bands in the 200 – 800 cm^{-1} region at 10 -ps as well as at -10 -ps delays, indicating that the photoproduct of the H77Y mutant has no Fe–His bond. If the ligand trans to CO in the CO-bound H77Y CoxA is a histidine, a band corresponding to the $\nu(\text{Fe–His})$ band should be observed. Its absence means that the CO-bound H77Y mutant has no axial histidine, supporting the ligation of His77 to the heme iron in the wild-type CO-bound CoxA.

In contrast, the presence of excess imidazole in the H77Y CoxA-CO solution resulted in the appearance of a new band at 222 cm^{-1} at 10 ps after photolysis (Figure 4c). The ν_7 band is also observed at 670 cm^{-1} , similar to that in Figure 1. The intensities of the two bands rapidly diminished with time, and the 222 cm^{-1} band became nondiscernible at 100 -ps delay (Figure 4d). Thus the disappearance of the 222 cm^{-1} band was faster than the case of the native $\nu(\text{Fe–His})$ band. The Im complexes of the mutants of Mb, sGC, and heme-bound heme oxygenase, in which axial His were replaced with a Gly or Ala residue, gave the Fe–Im stretching mode at 226 , 228 , and 221 cm^{-1} , respectively (21–23). The band observed at 222 cm^{-1} for the Im complex of the H77Y CoxA mutant, therefore, can be assigned to the $\nu(\text{Fe–Im})$ mode of the $5c$ high-spin imidazole complex. The presence of the

Table 1: Comparison of the Fe–His Stretching Frequencies in Various Heme Proteins

protein ^a	vibrational mode		ref
	$\nu(\text{Fe–His})$ (cm^{-1})	ν_4 (cm^{-1})	
sGC	204	1358	30
FixL*	209, 212	1355	32, 41, 42
CooA	211	1353	this work ^e
FixLN	212	1354	41, 42
CcO	214	1357	43–46
T-state HbA	215	1357	24, 47
HO-1	218	1354	48
Mb	220	1355	16, 29, 49–53
R-state HbA	221	nr ^b	24, 47
HRP	244, ^c 241 ^d	1357 ^c	28, 54, 55
CcP	247, ^c 234 ^d	1355, ^c 1360 ^d	25, 26, 56, 57
LPO	255	1357	58

^a Abbreviations: FixL*, soluble truncated domain of FixL; FixLN, heme domain of FixL; CcO, cytochrome *c* oxidase; HO-1, heme–heme oxygenase complex (isoform 1); HRP, horseradish peroxidase; CcP, cytochrome *c* peroxidase; LPO, lactoperoxidase. ^b Not reported. ^c Alkaline form. ^d Acid form. ^e Transiently observed just after CO photodissociation.

$\nu(\text{Fe–Im})$ mode in the RR spectra of H77Y CoxA with excess Im confirmed that exogenous Im resides at the site which otherwise His77 occupied in the wild-type CoxA-CO.

DISCUSSION

As clearly shown in the present results, His77 is the axial ligand in CO-bound CoxA, and CO displaces X of reduced CoxA. The $\nu(\text{Fe–His})$ frequency of the photodissociated CoxA provides us with structural information for the heme environments of CO-bound CoxA (13, 20). The $\nu(\text{Fe–His})$ bands have been observed for various $5c$ reduced hemoproteins in the region between 200 and 250 cm^{-1} , as summarized in Table 1. The important determinants of the $\nu(\text{Fe–His})$ frequency is the hydrogen-bonding status (15) and steric distortion (24) of the axial His. In cytochrome *c* peroxidase, the strong hydrogen bond between the axial His and Asp235 enhances the anionic character of the imidazole ring of the axial His, resulting in the higher $\nu(\text{Fe–His})$ frequency ($\sim 245\text{ cm}^{-1}$) (25). When this hydrogen bond is disrupted by the Asp235 \rightarrow Asn mutation, the frequency is shifted to a low frequency (205 cm^{-1}) (26, 27). The axial His of HRP has the same anionic character (28). In contrast, deoxy Mb, which has a weak hydrogen bond on the axial His, exhibits the $\nu(\text{Fe–His})$ mode around 220 cm^{-1} (29). The $\nu(\text{Fe–His})$ frequency of photodissociated CoxA at 211 cm^{-1} , therefore, reflects that the axial His is neutral and has no or very weak hydrogen bonds to other amino acids, supporting our previous conclusion (6) from the correlation between the $\nu(\text{Fe–C})$ and $\nu(\text{C–O})$ frequencies (11).

The effect of geometrical distortion of axial His due to strain from the protein on the $\nu(\text{Fe–His})$ frequency is most clearly seen in the difference between the T and R structures of deoxy Hb (24). It is also seen upon replacement of the axial His with glycine in the presence of exogenous imidazole, where the strain is relieved to increase the $\nu(\text{Fe–Im})$ frequency (21–23). The lower frequency in $\nu(\text{Fe–His})$ of CoxA than the $\nu(\text{Fe–Im})$ of the H77Y mutant in the presence of Im indicates that some strain is imposed on the Fe–His bond in CoxA. The relatively larger increase of $\nu(\text{Fe–Im})$

in H77Y CooA with imidazole [$\Delta\nu(\text{His}\rightarrow\text{Im}) = \nu(\text{Fe}-\text{Im}) - \nu(\text{Fe}-\text{His}) = 11 \text{ cm}^{-1}$] than those of Mb and heme oxygenase mutants [$\Delta\nu(\text{His}\rightarrow\text{Im}) = 6$ and 4 cm^{-1} , respectively] (21, 23) suggests that the strength of the strain on the Fe–His bond is larger in CooA.

It should be noted that other gas-sensing hemoproteins such as sGC and FixL also have low $\nu(\text{Fe}-\text{His})$ frequencies. The $\nu(\text{Fe}-\text{His})$ frequency of sGC is $203\text{--}204 \text{ cm}^{-1}$, suggestive of the presence of the severe strain in the Fe–His linkage (30). When nitric oxide binds to the heme iron, the Fe–His bond is broken, which triggers the activation of sGC (31). The weak Fe–His bond of sGC is suitable for intramolecular signal transduction via conformation changes initiated by dissociation of the axial ligand from the heme iron. The weak Fe–His bond was also reported for FixL, the $\nu(\text{Fe}-\text{His})$ of which was observed at 209 cm^{-1} (32). Although the signal transduction mechanism for CooA is supposed to be related to the structural alterations around the CO binding site, but not around the axial histidine site (2, 4, 6), the presence of strain in the Fe–His bond of CooA raises a possibility that a change in the Fe–His bond by CO binding plays some roles in signal transduction of CooA.

The weak Fe–His bond would also be related with the redox-dependent axial ligand exchange of CooA. The EPR and electronic absorption spectra of wild-type CooA indicate that the axial His is replaced with Cys75 upon the oxidation of heme iron to form Cys/X ligation (5, 7). Although the functional significance of the ligand exchange has not yet been clarified, the presence of strain in the Fe–His bond would facilitate the axial ligand exchange of CooA, which is one of the characteristic features in heme environments of CooA.

Another characteristic feature in CooA is the rapid recombination of CO to the heme iron. Our preliminary kinetic analysis showed that over 80% of the photoproducts rebind with CO within 200 ps, and its geminate yield was quite high (data not shown). Here the geminate rate constant for the CO rebinding was calculated by fitting the time course of the intensity of ν_4 with a single-exponential function. The obtained rate constant was $1.4 \times 10^{10} \text{ s}^{-1}$ (time constant = ~ 70 ps), which is much larger than those for other hemoproteins ($3\text{--}50 \times 10^6 \text{ s}^{-1}$) (33–35). Such a high geminate yield and the fast rate for the CO rebinding suggest that the interior volume of heme pocket of CooA is quite small. Extensive studies of ligand binding to Mb have revealed that the geminate yield and rate constant are largely affected by the location of the ligand dissociated from the iron (36). Inhibition of ligand movement after dissociation by placing a bulky amino acid residue in the heme pocket leads to a high geminate yield and a large rate constant, such as V68F mutants (37–40). This observation allows us to speculate that the heme pocket structure around CO in CooA is so crowded as to serve as a “cage” to trap CO.

In summary, we successfully detected the Fe–His stretching mode of photodissociated CooA at 211 cm^{-1} by using picosecond time-resolved resonance Raman spectroscopy. Since this band is absent in the H77Y mutant, we conclude that His77 is the axial ligand of CO-bound CooA and that the axial ligand trans to His77 is replaced with CO to activate CooA. The weak Fe–His bond and rapid geminate recombination of CO characterize the heme environmental structure of CO-bound CooA, which would be related to the activation

of CooA by CO.

ACKNOWLEDGMENT

We thank Dr. Satoshi Takahashi of Kyoto University for helpful discussions and suggestions.

REFERENCES

- Shelver, D., Kerby, R. L., He, Y. P., and Roberts, G. P. (1995) *J. Bacteriol.* 177, 2157–2163.
- Shelver, D., Kerby, R. L., He, Y., and Roberts, G. P. (1997) *Proc. Natl. Acad. Sci. U.S.A.* 94, 11216–11220.
- He, Y., Shelver, D., Kerby, R. L., and Roberts, G. P. (1996) *J. Biol. Chem.* 271, 120–123.
- Aono, S., Nakajima, H., Saito, K., and Okada, M. (1996) *Biochem. Biophys. Res. Commun.* 228, 752–756.
- Aono, S., Ohkubo, K., Matsuo, T., and Nakajima, H. (1998) *J. Biol. Chem.* 273, 25757–25764.
- Uchida, T., Ishikawa, H., Takahashi, S., Ishimori, K., Morishima, I., Ohkubo, K., Nakajima, H., and Aono, S. (1998) *J. Biol. Chem.* 273, 19988–19992.
- Shelver, D., Thorsteinsson, M. V., Kerby, R. L., Chung, S. Y., Roberts, G. P., Reynolds, M. F., Parks, R. B., and Burstyn, J. N. (1999) *Biochemistry* 38, 2669–2678.
- Vogel, K. M., Spiro, T. G., Shelver, D., Thorsteinsson, M. V., and Roberts, G. P. (1999) *Biochemistry* 38, 2679–2687.
- Weber, I. T., and Steitz, T. A. (1987) *J. Mol. Biol.* 198, 311–326.
- Aono, S., Matsuo, T., Shimono, T., Ohkubo, K., Takasaki, H., and Nakajima, H. (1997) *Biochem. Biophys. Res. Commun.* 240, 783–786.
- Yu, N. T., Kerr, E. A., Ward, B., and Chang, C. K. (1983) *Biochemistry* 22, 4534–4543.
- Dhawan, I. K., Shelver, D., Thorsteinsson, M. V., Roberts, G. P., and Johnson, M. K. (1999) *Biochemistry* 38, 12805–12813.
- Mizutani, Y., and Kitagawa, T. (1997) *Science* 278, 443–446.
- Uesugi, Y., Mizutani, Y., and Kitagawa, T. (1997) *Rev. Sci. Instrum.* 68, 4001–4008.
- Kitagawa, T. (1988) in *Biological Applications of Raman Spectroscopy* (Spiro, T. G., Ed.) Vol. III, pp 97–131, John Wiley & Sons, New York.
- Kitagawa, T., Kyogoku, Y., Iizuka, T., and Ikeda-Saito, M. (1976) *J. Am. Chem. Soc.* 98, 5169–5173.
- Hurst, J. K., Loehr, T. M., Curnutte, J. T., and Rosen, H. (1991) *J. Biol. Chem.* 266, 1627–1634.
- Smulevich, G., Bjerrum, M. J., Gray, H. B., and Spiro, T. G. (1994) *Inorg. Chem.* 33, 4639–4634.
- Anderton, C. L., Hester, R. E., and Moore, J. N. (1995) *Biochim. Biophys. Acta* 1253, 1–4.
- Dasgupta, S., Spiro, T. G., Johnson, C. K., Dalickas, G. A., and Hochstrasser, R. M. (1985) *Biochemistry* 24, 5295–5297.
- Franzen, S., Bohn, B., Poyart, C., DePhillis, G., Boxer, S. G., and Martin, J. L. (1995) *J. Biol. Chem.* 270, 1718–1720.
- Zhao, Y., Schelvis, J. P., Babcock, G. T., and Marletta, M. A. (1998) *Biochemistry* 37, 4502–4509.
- Wilks, A., Sun, J., Loehr, T. M., and Ortiz de Montellano, P. R. (1995) *J. Am. Chem. Soc.* 117, 2925–2926.
- Nagai, K., Kitagawa, T., and Morimoto, H. (1980) *J. Mol. Biol.* 136, 271–289.
- Hashimoto, S., Teraoka, J., Inubushi, T., Yonetani, T., and Kitagawa, T. (1986) *J. Biol. Chem.* 261, 11110–11118.
- Smulevich, G., Mauro, J. M., Fishel, L. A., English, A. M., Kraut, J., and Spiro, T. G. (1988) *Biochemistry* 27, 5477–5485.
- Spiro, T. G., Smulevich, G., and Su, C. (1990) *Biochemistry* 29, 4497–4508.
- Teraoka, J., and Kitagawa, T. (1981) *J. Biol. Chem.* 256, 3969–3977.
- Kitagawa, T., Nagai, K., and Tsubaki, M. (1979) *FEBS Lett.* 104, 376–378.
- Deinum, G., Stone, J. R., Babcock, G. T., and Marletta, M. A. (1996) *Biochemistry* 35, 1540–1547.

31. Stone, J. R., and Marletta, M. A. (1994) *Biochemistry* 33, 5636–5640.
32. Tamura, K., Nakamura, H., Tanaka, Y., Oue, S., Tsukamoto, K., Nomura, M., Tsuchiya, T., Adachi, S., Takahashi, S., Iizuka, T., and Shiro, Y. (1996) *J. Am. Chem. Soc.* 118, 9434–9435.
33. Hofrichter, J., Sommer, J. H., Henry, E. R., and Eaton, W. A. (1983) *Proc. Natl. Acad. Sci. U.S.A.* 80, 2235–2239.
34. Campbell, B. F., Magde, D., and Sharma, V. S. (1984) *J. Mol. Biol.* 179, 143–150.
35. Gibson, Q. H., Olson, J. S., McKinnie, R. E., and Rohlf, R. J. (1986) *J. Biol. Chem.* 261, 10228–10239.
36. Olson, J. S., and Phillips, G. N., Jr. (1996) *J. Biol. Chem.* 271, 17593–17596.
37. Carver, T. E., Rohlf, R. J., Olson, J. S., Gibson, Q. H., Blackmore, R. S., Springer, B. A., and Sligar, S. G. (1990) *J. Biol. Chem.* 265, 20007–20020.
38. Gibson, Q. H., Regan, R., Elber, R., Olson, J. S., and Carver, T. E. (1992) *J. Biol. Chem.* 267, 22022–22034.
39. Quillin, M. L., Li, T., Olson, J. S., Phillips, G. N., Jr., Dou, Y., Ikeda-Saito, M., Regan, R., Carlson, M., Gibson, Q. H., Li, H., and Elber, R. (1995) *J. Mol. Biol.* 245, 416–436.
40. Sugimoto, T., Unno, M., Shiro, Y., Dou, Y., and Ikeda-Saito, M. (1998) *Biophys. J.* 75, 2188–2194.
41. Rodgers, K. R., Lukat-Rodgers, G. S., and Barron, J. A. (1996) *Biochemistry* 35, 9539–9548.
42. Lukat-Rodgers, G. S., and Rodgers, K. R. (1997) *Biochemistry* 36, 4178–4187.
43. Argade, P. V., Ching, Y. C., and Rousseau, D. L. (1984) *Science* 225, 329–331.
44. Sone, N., Ogura, T., and Kitagawa, T. (1986) *Biochim. Biophys. Acta* 850, 139–145.
45. Ogura, T., Hon-nami, K., Oshima, T., Yoshikawa, S., and Kitagawa, T. (1983) *J. Am. Chem. Soc.* 105, 7781–7783.
46. Choi, S., Lee, J. J., Wei, Y. H., and Spiro, T. G. (1983) *J. Am. Chem. Soc.* 105, 3692–3707.
47. Friedman, J. M., Stepnoski, R. A., Stavola, M., Ondrias, M. R., and Cone, R. L. (1982) *Biochemistry* 21, 2022–2028.
48. Takahashi, S., Wang, J., Rousseau, D. L., Ishikawa, K., Yoshida, T., Takeuchi, N., and Ikeda-Saito, M. (1994) *Biochemistry* 33, 5531–5538.
49. Kincaid, J., Stein, P., and Spiro, T. G. (1979) *Proc. Natl. Acad. Sci. U.S.A.* 76, 549–552.
50. Choi, S., Spiro, T. G., Langry, K. C., Budd, D. L., and La Mar, G. N. (1982) *J. Am. Chem. Soc.* 104, 4345–4351.
51. Argade, P. V., Sassaroli, M., Rousseau, D. L., Inubushi, T., Ikeda-Saito, M., and Lapidot, A. (1984) *J. Am. Chem. Soc.* 106, 6593–6596.
52. Rousseau, D. L., and Friedman, J. M. (1988) in *Biological Applications of Raman Spectroscopy* (Spiro, T. G., Ed.) Vol. III, John Wiley & Sons, New York.
53. Wells, A. V., Sage, J. T., Morikis, D., Champion, P. M., Chiu, M. L., and Sligar, S. G. (1991) *J. Am. Chem. Soc.* 113, 9655–9660.
54. Yamamoto, T., Palmer, G., Gill, D., Salmeen, I. T., and Remi, L. (1973) *J. Biol. Chem.* 248, 5211–5213.
55. Alden, R. G., and Ondrias, M. R. (1985) *J. Biol. Chem.* 260, 12194–12197.
56. Dasgupta, S., Rousseau, D. L., Anni, H., and Yonetani, T. (1989) *J. Biol. Chem.* 264, 652–662.
57. Wang, J. L., Boldt, N. J., and Ondrias, M. R. (1992) *Biochemistry* 31, 867–878.
58. Manthey, J. A., Boldt, N. J., Bocian, D. F., and Chan, S. I. (1986) *J. Biol. Chem.* 261, 6734–6741.

BI0011476